Springer

KSME

Journal of Mechanical Science and Technology 24 (12) (2010) 2431~2440
www.springerlink.com/content/1738-494x
DOI 10.1007/s12206-010-0913-3

Frequency-domain computation of inflow broadband noise due to interaction of a rectilinear cascade of flat plates with incident turbulence †

Dingbing Wei and Cheolung Cheong*

School of Mechanical Engineering, Pusan National University, Korea

(Manuscript Received June 10, 2010; Revised August 20, 2010; Accepted August 24, 2010)

Abstract

This paper deals with the broadband noise due to the interaction between convected turbulent gusts and a rectilinear cascade of flat plates bounded by two parallel walls. An analytic formulation for the acoustic power spectrum due to this turbulence-cascade interaction is derived, which can be used to assess the effects of the span-wise wavenumber components of ingesting turbulent gust on the overall acoustic power spectrum. This three-dimensional theory is based on the two-dimensional theory of Cheong et al. (2006, 2009). The three-dimensional model is shown to provide a close fit to the measured spectrum of rotor-stator interaction. The predictions using this three-dimensional model are also compared with those using the previous two-dimensional model by Cheong et al. (2006; 2009). Through this comparison, it is found that the contributions to the acoustic power of the span-wise wavenumber components of incident turbulent gust are increased as the frequency is augmented, which is mainly due to three-dimensional dispersion-relation characteristics of acoustic waves. This implies that the number of incident turbulent gust modes directly involved in generating cut-on acoustic waves increases as the frequency increases. Therefore, in the lower frequency range, three-dimensional acoustic power is less than its corresponding two-dimensional one, whereas, as the frequency increases, the three-dimensional acoustic power spectrum closely follows those of two-dimension. The formulation is also used to make a parametric study about the effects on the power spectrum of the blade number, stagger angle, gap-chord ratio, and Mach number.

Keywords: Broadband inflow noise; Fan noise; Aerodynamic noise; Turbulent gust; A rectilinear cascade of flat plates

1. Introduction

Aircraft today have become a widely-used traffic tool. It is critical for aero-engine manufacturers to develop quieter products. The aero-engine noise consists of fan noise, compressor noise, turbine noise, combustion noise, jet noise, etc. Among them, fan noise is the most significant part which can be further categorized into tonal noise and broadband noise. Fan tonal noise has now been lessened with fewer blades and lower rotation speed of future Ultra High Bypass Ratio engine-design. Therefore, fan broadband noise becomes the major contributor to the overall noise of aero-engine.

Fan broadband noise may be categorized into self noise and inflow noise. Self noise is due to the interaction between the turbulence generated in the boundary layer on the blade surface and the trailing edge. It is the noise produced by the airfoil situated in a smooth, non-turbulent in-flow. The self noise may be further divided into five categories based on its generation mechanism [1]. Broadband inflow noise originates from the interaction between inflow turbulence with rotors or stators. The ingested turbulence may be atmospheric turbulence, boundary layer turbulence and rotor-wake turbulence. However, it is known that the inflow broadband noise due to interaction of the rotor wakes and stators has a greater contribution to overall noise levels.

Many researches on fan broadband inflow noise have been carried out. Smith [2] developed the first theory based on classical aerodynamic vortex theory to predict the unsteady blade loading and the acoustic field upstream and downstream of a two-dimensional cascade of flat-plate airfoils perfectly aligned with a uniform mean flow. Whitehead [3] developed the LINSUB code to calculate the unsteady two-dimensional linearized subsonic flow in a cascade, using the theory developed by Smith. Using the Wiener-Hopf techniques, Glegg [4] has given an analytic expression for the unsteady blade loading, acoustic mode amplitude, and sound power output of a three-dimensional rectilinear cascade of blades with finite chord excited by a three-dimensional vortical gust and investigated the effects of blade sweep and oblique gust arrival angles. Using the similar theory, Hanson and Horan [5] also did re-

† This paper was recommended for publication in revised form by Associate Editor Yeon June Kang

* Corresponding author. Tel.: +82 51 510 2311, Fax.: +82 51 514 7460
E-mail address: ccheong@pusan.ac.kr

search about the broadband noise due to turbulence/cascade interaction. Later, Hanson [6] extended the research to investigate the influence of lean and sweep on noise of cascades with turbulent inflow. Cheong et al. [7] generalized Smith's theory to broadband noise, defined the concept of critical frequency, and made a full investigation on modal acoustic power (MAP). Cheong et al. [8] also made a modal-decomposition analysis to assess the effects of its sub-components on modal acoustic power.

Extending the previous works [7, 8] based on two-dimensional theory, this paper investigates the broadband noise due to the interaction between convected turbulent gusts and a rectilinear cascade of flat plates bounded by two parallel walls. An analytic formulation for the acoustic power spectrum due to this three-dimensional turbulence-cascade interaction is derived. The three-dimensional model is shown to provide a close fit to the measured spectrum of rotor-stator interaction. The predictions using this three-dimensional model are also compared with those using the previous two-dimensional model by Cheong et al. [7, 8]. Through this comparison, it is found that the contribution to the acoustic power of the span-wise wave number components of incident turbulent gust is increased as the frequency is augmented, which is mainly due to three-dimensional dispersion-relation characteristics of acoustic waves. The main contribution of this work is to make clear the effects of the span-wise wave number components of ingesting turbulent gust on the overall acoustic power spectrum, which reveals that the number of incident turbulent gust modes directly involved in generating cut-on acoustic waves increases as the frequency increases. Therefore, in the lower frequency range, three-dimensional acoustic power is less than its corresponding two-dimensional one, whereas, as the frequency increases, three-dimensional acoustic power spectrum closely follows those of two-dimensional. The formulation is also used to make a parametric study on the effects on the power spectrum of the blade number, stagger angle, gap-chord ratio, and Mach number.

2. Response of rectilinear cascade to incident gusts

The cascade geometry investigated in this paper and its co-ordinate systems are shown in Fig. 1. A three-dimensional cascade of flat-plate airfoils with stagger angle θ is assumed to be located in a two-dimensional uniform flow moving in the direction parallel to the chord, i.e., with zero incident angle. Homogeneous isotropic turbulence is assumed to be convected with mean flow of speed, A, as a "frozen gust pattern". In Fig. 1, (x_1, x_2, x_3) is the unwrapped duct coordinate system, and (y_1, y_2, y_3) is the cascade-fixed coordinate system.

The linearized three-dimensional equations of momentum and continuity are

$$\frac{\partial \rho}{\partial t}+U\frac{\partial \rho}{\partial x_1}+V\frac{\partial \rho}{\partial x_2}+W\frac{\partial \rho}{\partial x_3}+\rho_0\left(\frac{\partial u}{\partial x_1}+\frac{\partial v}{\partial x_2}+\frac{\partial w}{\partial x_3}\right)=0,$$

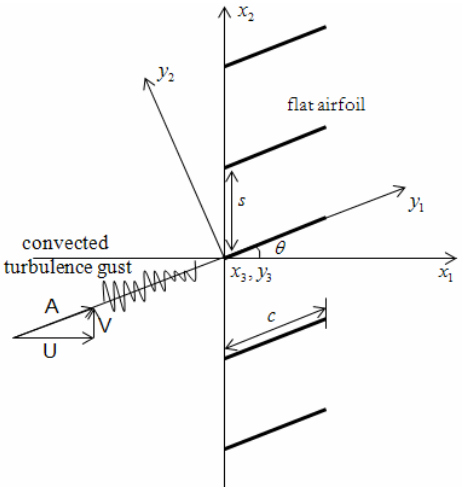

Fig. 1. The cascade geometry and the convected turbulent gust. x_3 and y_3 coordinates are coming directly out of the page.

$$\begin{aligned}
&\frac{\partial u}{\partial t}+U\frac{\partial u}{\partial x_1}+V\frac{\partial u}{\partial x_2}+W\frac{\partial u}{\partial x_3}+\frac{1}{\rho_0}\frac{\partial p}{\partial x_1}=0,\\
&\frac{\partial v}{\partial t}+U\frac{\partial v}{\partial x_1}+V\frac{\partial v}{\partial x_2}+W\frac{\partial v}{\partial x_3}+\frac{1}{\rho_0}\frac{\partial p}{\partial x_2}=0,\\
&\frac{\partial w}{\partial t}+U\frac{\partial w}{\partial x_1}+V\frac{\partial w}{\partial x_2}+W\frac{\partial w}{\partial x_3}+\frac{1}{\rho_0}\frac{\partial p}{\partial x_3}=0,
\end{aligned} \tag{1}$$

where U, V and W are the mean velocities in the x_1, x_2 and x_3 directions, respectively; u, v and ω are the corresponding unsteady velocity perturbations; ρ_0 and ρ are the mean and perturbation densities, respectively. The flow is assumed to be isentropic, so that

$$\left(\frac{\partial p}{\partial \rho}\right)_S=\frac{dp}{d\rho}=a^2, \tag{2}$$

where a is the speed of sound. For harmonic space and time dependence, the perturbation quantities may be written as

$$\begin{vmatrix} u\\ v\\ w\\ p \end{vmatrix}=\begin{vmatrix} \bar{u}\\ \bar{v}\\ \bar{w}\\ \bar{p} \end{vmatrix}\exp i(\omega t+\alpha x_1+\beta x_2+\gamma x_3), \tag{3}$$

in which $\bar{u}$, $\bar{v}$, $\bar{w}$ and $\bar{p}$ are constant complex amplitudes and α, β and γ are wave numbers. Using Eqs. (2) and (3), Eq. (1) becomes:

$$\begin{vmatrix} H & a^2\alpha\rho_0 & a^2\beta\rho_0 & a^2\gamma\rho_0\\ \alpha/\rho_0 & H & 0 & 0\\ \beta/\rho_0 & 0 & H & 0\\ \gamma/\rho_0 & 0 & 0 & H \end{vmatrix}\times\begin{vmatrix} \bar{p}\\ \bar{u}\\ \bar{v}\\ \bar{w} \end{vmatrix}=0, \tag{4}$$

where $H=\omega+U\alpha+V\beta+W\gamma$.

The condition for the existence of a non-trivial solution of Eq. (4) is

$$H^2 \times \left| H^2 - a^2(\alpha^2 + \beta^2 + \gamma^2) \right| = 0 , \quad (5)$$

where $H = \omega + U\alpha + V\beta + W\gamma$.

Two different physical phenomena are embodied in Eq. (5), acoustic waves and vorticity waves, and these will be considered separately. The acoustic waves satisfy the relations:

$$(\omega + U\alpha + V\beta + W\gamma)^2 - a^2(\alpha^2 + \beta^2 + \gamma^2) = 0 . \quad (6)$$

Eq. (6) can be expressed in the form:

$$\alpha = \frac{U(\omega + V\beta + W\gamma) \pm a\sqrt{(\omega + V\beta + W\gamma)^2 - (a^2 - U^2)(\beta^2 + \gamma^2)}}{a^2 - U^2} \quad (7)$$

with the assumption that β and γ are real. The two values of α correspond one to upstream going and the other to downstream going perturbations. Vorticity wave gives the following relation:

$$(\omega + U\alpha + V\beta + W\gamma)^2 = 0 . \quad (8)$$

Eq. (8) can be rearranged for α,

$$\alpha = -\frac{\omega + V\beta + W\gamma}{U} . \quad (9)$$

Disturbances of this type propagate without associated pressure fluctuations.

In this paper, the mean flow velocity in x_3-direction, W, must be zero under the considered cascade geometry to satisfy the boundary condition given in Fig. 2. A single wave number component (k_1, k_2, k_3) has a phase angle σ between adjacent blades separated by a gap s given by

$$\alpha = (k_1 \sin\theta + k_2 \cos\theta)s . \quad (10)$$

The phase angle σ between adjacent blades of r-th acoustic wave generated from the cascade due to a single wave number component of vorticity (k_1, k_2, k_3) is of the form $\beta_r s = \sigma - 2\pi r$. So the acoustic circumferential wave number β_r of the r-th acoustic wave is given by

$$\beta_r = \frac{(k_1 \sin\theta + k_2 \cos\theta)s - 2\pi r}{s} . \quad (11)$$

Then, the solution for axial wave number can be expressed in terms of β_r, k_3 and ω as:

$$\alpha_r(k_3) = \frac{M_1(\frac{\omega}{a} + M_2\beta_r) \pm \sqrt{(\frac{\omega}{a} + M_1\beta_r)^2 - (1 - M_1^2)(\beta_r^2 + k_3^2)}}{1 - M_1^2} \quad (12)$$

Here, the wavenumber of acoustic wave, γ, in the span-wise direction is replaced by the incident wavenumber of vorticity wave, k_3, because the rectilinear cascade is uniform in the x_3-direction.

The acoustic pressure amplitude of the cascade impinged by a harmonic gust can be obtained by following the procedure presented by Smith [2]. For a harmonic gust of the form,

$$w(y_1, y_2, y_3, t) = w_0 e^{i[k_1(y_1 - At) + k_2 y_2 + k_3 y_3]} . \quad (13)$$

The acoustic pressure upstream and downstream of the cascade is of the form,

$$p^{\pm}(x_1, x_2, x_3, t) = \rho_0 A w_0 e^{ik_3 x_3} \sum_{r=-\infty}^{\infty} R_r^{\pm}(k_1, k_2) e^{i(k_1 At + \alpha_r^{\pm}(k_3)x_1 + \beta_r x_2)} \quad (14)$$

where R_r is defined as the cascade response function, which is completely defined by the parameters of s/c, θ, M, λ and σ.

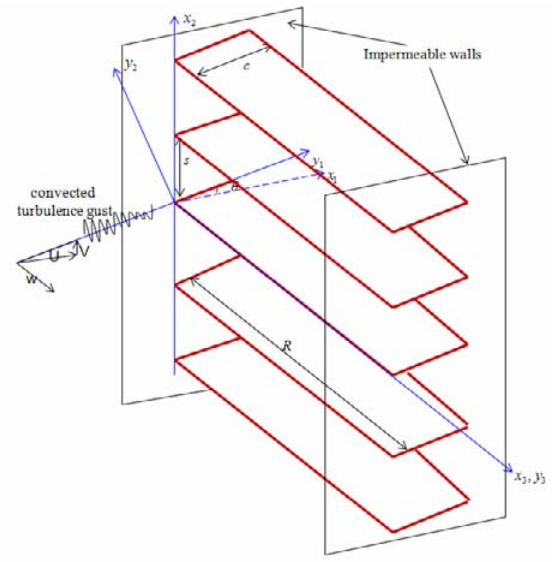

Fig. 2. The 3-D cascade geometry and the convected turbulent gust.

3. Extension to broadband acoustic power formulation

Using the Fourier transform, the sound radiation due to an incident sinusoidal vortical gust can be extended to broadband turbulent velocity distributions. Assuming that turbulence velocities are much smaller than mean velocities, Taylor's hypothesis can be applied to treat the turbulence as a "frozen gust pattern" which is convected with the mean velocities. Then, straightforward extension of the formula for the acoustic pressure for radiation due to an incident three-dimensional sinusoidal vortical gust leads to the expression for broadband acoustic pressure from a cascade subject to the impinging turbulent gust, in the form,

$$p^{\pm}(x_1,x_2,x_3,t)=\rho_0 A\int_{-\infty}^{\infty}\int_{-\infty}^{\infty}\int_{-\infty}^{\infty}\hat{\hat{\hat{w}}}_D(k_1,k_2,k_3)\times e^{ik_3x_3}\sum_{r=-\infty}^{\infty}R_r^{\pm}(k_1,k_2)e^{i(k_1At+\alpha_r^{\pm}(k_3)x_1+\beta_r x_2)}dk_1dk_2dk_3 \quad (15)$$

where $\hat{\hat{\hat{w}}}_D(k_1,k_2,k_3)$ is the three-dimensional turbulence wave number spectrum of the turbulence velocity evaluated in the moving reference frame. Taking the Fourier transform of Eq. (15) with respect to t, we can transfer the acoustic pressure from time domain to frequency domain in this form,

$$p_{\mathrm{T}}^{\pm}(x_1,x_2,x_3,\omega)=\rho_0\int_{-\infty}^{\infty}\int_{-\infty}^{\infty}\int_{-\infty}^{\infty}\hat{\hat{\hat{w}}}_D(k_1,k_2,k_3)\times e^{ik_3x_3}\sum_{r=-\infty}^{\infty}R_r^{\pm}(k_1,k_2)e^{i(\alpha_r^{\pm}(k_3)x_1+\beta_r x_2)}\times\left\{\frac{A}{2\pi}\int_{-T}^{T}e^{i(k_1A+\omega)t}dt\right\}dk_1dk_2dk_3 \quad (16)$$

The term within the curly brackets corresponds to a delta-function $\delta(k_1-K_1)$ as T goes to infinity, where $K_1=-\omega/A$. Only the component of the turbulence with an axial wave number k_1 equal to K_1 therefore contributes to acoustic pressure. Integration over the axial wave number is therefore trivial and Eq. (16) becomes:

$$\tilde{p}_{\mathrm{T}}^{\pm}(x_1,x_2,x_3,\omega)=\rho_0\int_{-\infty}^{\infty}\int_{-\infty}^{\infty}\hat{\hat{\hat{w}}}_D(\mathrm{K}_1,k_2,k_3)\times e^{ik_3x_3}\sum_{r=-\infty}^{\infty}R_r^{\pm}(\mathrm{K}_1,k_2)e^{i(\alpha_r^{\pm}(k_3)x_1+\beta_r x_2)}dk_2dk_3 \quad (17)$$

Substituting Eq. (17) into the momentum equation, we can get the acoustic velocities in the axial and gap-wise directions, respectively:

$$\tilde{u}_T^{\pm}(x_1,x_2,x_3,\omega)=\rho_0\int_{-\infty}^{\infty}\int_{-\infty}^{\infty}\hat{\hat{\hat{w}}}_D(\mathrm{K}_1,k_2,k_3)e^{ik_3x_3}\times\sum_{r=-\infty}^{\infty}\frac{-\alpha_r^{\pm}(k_3)R_r^{\pm}(\mathrm{K}_1,k_2)e^{i(\alpha_r^{\pm}(k_3)x_1+\beta_r x_2)}}{\rho_0(\omega+U\alpha_r^{\pm}(k_3)+V\beta_r)}dk_2dk_3 \quad (18)$$

$$\tilde{v}_T^{\pm}(x_1,x_2,x_3,\omega)=\rho_0\int_{-\infty}^{\infty}\int_{-\infty}^{\infty}\hat{\hat{\hat{w}}}_D(\mathrm{K}_1,k_2,k_3)e^{ik_3x_3}\times\sum_{r=-\infty}^{\infty}\frac{-\beta_r^{\pm}R_r^{\pm}(\mathrm{K}_1,k_2)e^{i(\alpha_r^{\pm}(k_3)x_1+\beta_r x_2)}}{\rho_0(\omega+U\alpha_r^{\pm}(k_3)+V\beta_r)}dk_2dk_3. \quad (19)$$

3.1 Acoustic power spectrum

To calculate the acoustic power spectrum, the instantaneous acoustic intensity vector for sound propagation in a uniform mean velocity A is required, which formula is given by Goldstein [9] as below:

$$I^{\pm}(\omega)=\lim_{T\to\infty}\frac{2\pi}{T}\mathrm{Re}\left\{\left(\frac{\tilde{p}_T^{\pm}(x_1,x_2,x_3,\omega)}{\rho_0}+U\tilde{u}_T^{\pm}(x_1,x_2,x_3,\omega)+V\tilde{v}_T^{\pm}(x_1,x_2,x_3,\omega)\right)\times\left(\rho_0\tilde{u}_T^{\pm *}(x_1,x_2,x_3,\omega)+\frac{U\tilde{p}_T^{\pm *}(x_1,x_2,x_3,\omega)}{c_0^2}\right)\right\} \quad (20)$$

Substituting Eqs. (17)-(19) into (20) leads to the formula for the intensity spectrum as:

$$I^{\pm}(x,\omega)=\rho_0\int_{-\infty}^{\infty}\int_{-\infty}^{\infty}\int_{-\infty}^{\infty}\int_{-\infty}^{\infty}\lim_{T\to\infty}\frac{2\pi}{T}E\left[\hat{\hat{\hat{w}}}_D(K_1,k_2,k_3)\hat{\hat{\hat{w}}}_D^{*}(K_1',k_2',k_3')\right]\sum_{r=-\infty}^{\infty}\sum_{r'=-\infty}^{\infty}\mathrm{Re}\left\{\frac{\omega(-\alpha_r^{\pm}(k_3)^{*}+M_1(\omega/a+M_1\alpha_{r'}^{\pm}(k_3)^{*}+M_2\beta_{r'}))}{c_0^2(k+M_1\alpha_r^{\pm}(k_3)+M_2\beta_r)(k+M_1\alpha_{r'}^{\pm}(k_3)^{*}+M_2\beta_{r'})}\times e^{i(k_3-k_3')x_3}\right.$$
$$\left.R_r^{\pm}(K_1,k_2)R_{r'}^{\pm *}(K_1,k_2')\times e^{i((\alpha_r^{\pm}(k_3)-\alpha_{r'}^{\pm}(k_3)^{*})x_1+(\beta_r-\beta_{r'})x_2)}\right\}dk_3dk_3'dk_2dk_2' \quad (21)$$

Assuming that the upwash velocity $\hat{\hat{\hat{w}}}_D$ is a statistically random variable and that the velocities at different wave numbers are uncorrelated, Amiet [10] shows that

$$\lim_{T\to\infty}\frac{2\pi}{T}E\left[\hat{\hat{\hat{W}}}_D(K_1,k_2,k_3)\hat{\hat{\hat{W}}}_D^{*}(K_1,k_2,k_3)\right],=A\delta(k_2-k_2')\delta(k_3-k_3')\phi_{WW}(K_1,k_2,k_3) \quad (22)$$

where $\Phi_{ww}(k_1,k_2,k_3)$ is the turbulence velocity wave number spectrum evaluated in the moving reference system. Inserting Eq. (22) into (21) and performing integrations over k_2' and k_3' leads to

$$I^{\pm}(x,\omega)=\rho_0 M\int_{-\infty}^{\infty}\int_{-\infty}^{\infty}\phi_{ww}(K_1,k_2,k_3)\sum_{r=-\infty}^{\infty}\sum_{r'=-\infty}^{\infty}\mathrm{Re}\left\{\frac{k(-\alpha_{r'}^{\pm}(k_3)^{*}+M_1(k+M_1\alpha_{r'}^{\pm}(k_3)^{*}+M_2\beta_{r'}))}{(k+M_1\alpha_r^{\pm}(k_3)^{*}+M_2\beta_r)(k+M_1\alpha_{r'}^{\pm}(k_3)^{*}+M_2\beta_{r'})}R_r^{\pm}(K_1,k_2)R_{r'}^{\pm *}(K_1,k_2)\right.$$
$$\left.e^{i\left((\alpha_r^{\pm}(k_3)-\alpha_{r'}^{\pm}(k_3)^{*})x_1+(\beta_r-\beta_{r'})x_2\right)}dk_2dk_3\right\} \quad (23)$$

Integrating the above Eq. (23) in the x_2-x_3 plane over an area of $Bs\times R$, we can get the acoustic power. Since the gap-wise direction wave numbers β_r and β_r' are periodic over a distance Bs, this integral is of the form

$$\int_0^R\int_0^{Bs}\exp(i(\beta_r-\beta_{r'})x_2)dx_2dx_3=RBs\delta_{rr'}, \quad (24)$$

where the Kronecker delta function $\delta_{rr'}$ enables the r' summation in Eq. (23) to be eliminated. Therefore, the acoustic power spectrum can be expressed as

$$P^{\pm}(\omega)=\rho_0 MRBs\int_{-\infty}^{\infty}\int_{-\infty}^{\infty}\phi_{ww}(K_1,k_2,k_3)\sum_{r=-\infty}^{\infty}\left|R_r^{\pm}(K_1,k_2,k_3)\right|^2\Im_r^{\pm}(k_3)dk_2dk_3$$

(25)

where $\Im_r^{\pm}(k_3)$ is non-dimensional acoustic power factor defined as

$$\Im_r^{\pm}(k_3)=\frac{kR_e\left\{-\alpha_r^{\pm}(k_3)^*+M_1\left(K+M_1\alpha_r^{\pm}(k_3)^*+M_2\beta_r\right)\right\}}{\left|K+M_1\alpha_r^{\pm}(k_3)^*+M_2\beta_r\right|^2} \tag{26}$$

Because of the periodicity of the turbulence spectrum in the x_2 direction, we can use Fourier series instead of the above Fourier integrals. So, the above Fourier integral over k_2 can be converted to Fourier series with the fundamental spatial frequency equal to $2\pi/Bs$. The wave numbers in the x_2 direction are therefore integer multiples of the fundamental spatial frequency and equal to

$$\beta=\frac{2\pi}{\mathrm{BS}}m\,. \tag{27}$$

The turbulence wave numbers k_1 and k_2, defined in the blade-fixed coordinate (y_1,y_2,y_3), can be expressed in the cascade coordinate system (x_1,x_2,x_3), which leads to the following relation:

$$\frac{2\pi}{\mathrm{BS}}m=\mathrm{K}_1\sin\theta+k_{2,m}\cos\theta\,. \tag{28}$$

Eq. (28) can be rearranged in the explicit form for $k_{2,m}$:

$$k_{2,m}=\frac{2\pi m}{\mathrm{BS}\cos\theta}-K_1\tan\theta\,, \tag{29}$$

where m is defined as the vortical mode number in the gapwise direction.

Therefore, integration over k_2 at a constant frequency (or K_1) can be replaced by:

$$\int dk_2=\frac{2\pi}{\mathrm{BS}\cos\theta}\sum_{m=-\infty}^{\infty}\,. \tag{30}$$

Thus, Eq. (25) now turns into

$$P^{\pm}(\omega)=\frac{2\pi\rho_0 M}{\cos\theta}\int_{-\infty}^{\infty}\sum_{m=-\infty}^{\infty}\phi_{ww}\left(K_1,k_{2,m},k_3\right)\sum_{r=-\infty}^{\infty}\left|R_r^{\pm}\left(K_1,k_2\right)\right|^2\Im_r^{\pm}(k_3)dk_3 \tag{31}$$

Similar reasoning can be applied for the k_3 in the x_3 direction. The wave number in the x_3 direction is therefore integer multiples of the fundamental spatial mode and equal to

$$k_{3,j}=\frac{\pi j}{R}\,. \tag{32}$$

So, integration over k_3 can be replaced by:

$$\int dk_3=\frac{\pi}{\mathrm{R}}\sum_{j=-\infty}^{\infty}\,. \tag{33}$$

Thus, Eq. (31) can be rewritten in the form

$$P^{\pm}(\omega)=\frac{2\pi^2\rho_0 M}{R\cos\theta}\sum_{j=-\infty}^{\infty}\sum_{m=-\infty}^{\infty}\phi_{ww}\left(K_1,k_{2,m},k_{3,j}\right)\sum_{r=-\infty}^{\infty}\left|R_r^{\pm}\left(K_1,k_{2,m}\right)\right|^2\Im_{r,j}^{\pm}, \tag{34}$$

where

$$\Im_{r,j}^{\pm}=\frac{kR_e\left\{-\alpha_r^{\pm}(k_{3,j})^*+M_1\left(K+M_1\alpha_r^{\pm}(k_{3,j})^*+M_2\beta_r\right)\right\}}{\left|K+M_1\alpha_r^{\pm}(k_{3,j})^*+M_2\beta_r\right|^2} \tag{35}$$

Formula (34) shows that the radiated sound power spectrum is due to an infinite number of impinging vortical modes m and j, each of which generates upstream and downstream going acoustic waves. However, Eq. (34) is not efficient when calculating the spectrum of acoustic power because $R_r^{\pm}$ appears inside the three summations over the variables of m, r and j. A transformation of the summation indices can be used to move $R_r^{\pm}$ out from the three summation into a single summation at the expense of moving the turbulence spectrum Φ_{ww} under the three summations. Such an arrangement is advantageous since Φ_{ww} will normally be computed from a simple algebraic expression, whereas $R_r^{\pm}$ requires another infinite summation of the so-called "cascade waves" and the numerical computation of the upwash integral equation in Smith's theory. Since the basic spatial period of the flow is Bs, the acoustic wave number in x_2 direction must satisfy

$$\beta_l=\frac{2\pi}{Bs}l\,, \tag{36}$$

where l is the acoustic mode in x_2 direction. Inserting Eqs. (29) and (36) into Eq. (11), the *m*-th vortical wave number may be written in terms of the acoustic mode number l and the cascade scattering index r as

$$m=l+Br\,. \tag{37}$$

Inserting Eq. (37) into Eq. (29) gives

$$k_{2,l+Br}=\frac{2\pi}{B\mathrm{s}\cos\theta}(l+Br)-K_1\tan\theta\,. \tag{38}$$

By using Eq. (38), Eq. (34) can be rearranged as

$$P^{\pm}(\omega) = \frac{2\pi^2\rho_0 M}{R\cos\theta}\sum_{l=-\infty}^{\infty}\left|R_l^{\pm}\left(K_1,k_{2,\mathrm{mod}(l,B)}\right)\right|^2\sum_{j=-\infty}^{\infty}\sum_{r=-\infty}^{\infty}\Im_{r,j}^{\pm}\phi_{ww}\left(K_1,k_{2,l+Br},k_{3,j}\right) \quad (39)$$

3.2 Turbulence spectrum

For simplicity, we just consider the circumstance that the turbulence impinging on the stator is homogeneous and isotropic. Liepmann spectrum $\Phi_{ww}(k_1,k_2,k_3)$ is a very suitable model for wave number PSD. The spectrum for the fluctuation velocity normal to the chord is of the form below:

$$\phi_{ww}(k_1,k_2,k_3) = \frac{E(k)}{4\pi k^2}\left(1-\frac{k_2}{k}\right), \quad (40)$$

where $k=\sqrt{k_1^2+k_2^2+k_3^2}$ and $E(k)$ is the energy spectrum defined by:

$$E(k) = \frac{8\overline{w}^2\Lambda}{\pi}\frac{(\Lambda k)^4}{\left(1+(\Lambda k)^2\right)^3}. \quad (41)$$

In this formula, $\overline{w}^2$ is the mean square value of the turbulence velocity in the direction normal to the chord and Λ is the turbulence integral length scale. From the above Eqs. (40) and (41), we can get the spectrum $\phi_{ww}(k_1,k_2,k_3)$:

$$\phi_{ww}(k_1,k_2,k_3) = \frac{2\overline{w}^2\Lambda^3}{\pi^2}\frac{\Lambda^2\left(k_1^2+k_3^2\right)}{\left(1+\Lambda^2\left(k_1^2+k_2^2+k_3^2\right)\right)^3}. \quad (42)$$

3.3 Cut-on condition

Eq. (39) defines the acoustic power spectrum due to an infinite summation over the acoustic mode number l. However, if we consider only the propagating wave components in Eq. (39), the infinite summation over l can be reduced to a finite frequency range. In a subsonic flow, $W<a$, propagating acoustic modes correspond to real values of $\alpha_r^{\pm}$, which occur over the range of β_l given by

$$\frac{kM_2-\sqrt{(1-M_1^2)\left[\left(M^2-1\right)\gamma^2+k^2\right]}}{1-M^2} \le \beta_l \le \frac{kM_2+\sqrt{(1-M_1^2)\left[\left(M^2-1\right)\gamma^2+k^2\right]}}{1-M^2}. \quad (43)$$

We use $L_{\max}$ and $L_{\min}$ to denote the maximum and minimum integers of acoustic mode number l satisfying the upper and lower inequality of Eq. (43). Eq(39) can now be written as

Table ction.

Mate

M	R
0.5	0.8

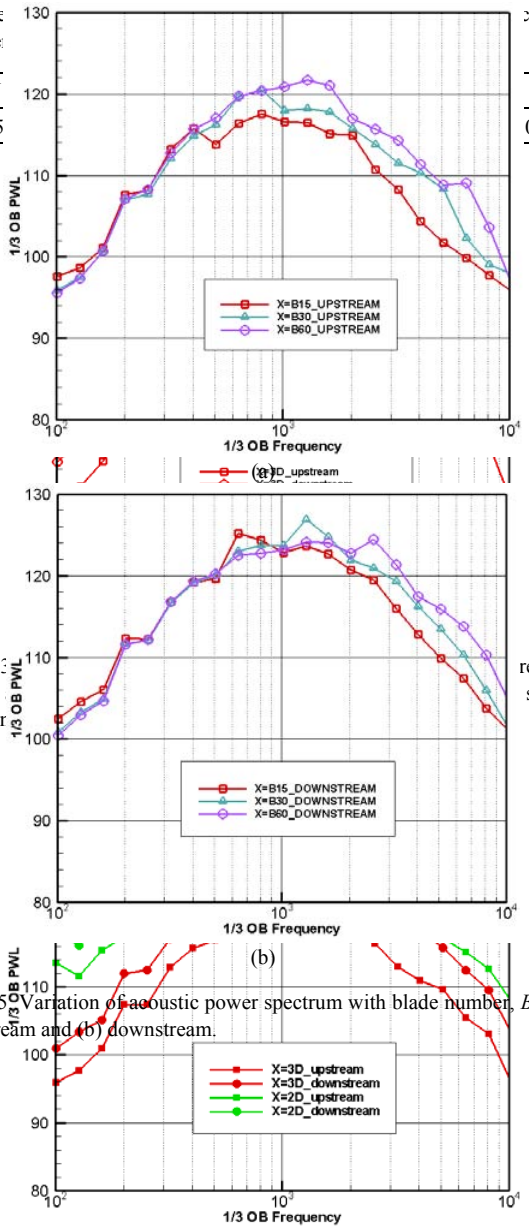

Fig. 3 redictions scale and ir

Fig. 5 Variation of acoustic power spectrum with blade number, B. (a) upstream and (b) downstream.

Fig. 4. Comparison of acoustic power spectra predicted using the present three-dimensional model with the two-dimensional models of Cheong et al. [7, 8]

$$P^{\pm}(\omega) = \frac{2\pi^2\rho_0 M}{R\cos\theta}\sum_{l=L_{\min}}^{L_{\max}}\left|R_l^{\pm}\left(K_1,k_{2,\mathrm{mod}(l,B)}\right)\right|^2 \sum_{j=-\infty}^{\infty}\sum_{r=-\infty}^{\infty}\Im_{r,j}^{\pm}\phi_{ww}\left(K_1,k_{2,l+Br},k_{3,j}\right), \quad (44)$$

where the range of r and j is also selected to ensure the cut-on condition and convergence, respectively. The broadband sound power over the frequency range $\omega_L \le \omega \le \omega_H$ can therefore be integrated as

$\Pi^{\pm} =$

$\sum_{j=-\infty}^{\infty}\sum_{r=-\infty}^{\infty}$

The pre

bels as a p

$PWL^{\pm}$ =

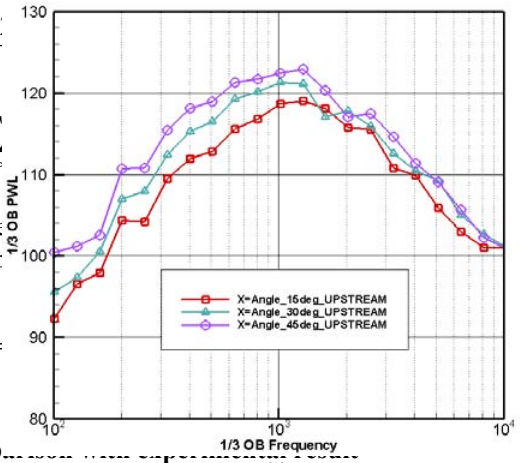

(a)

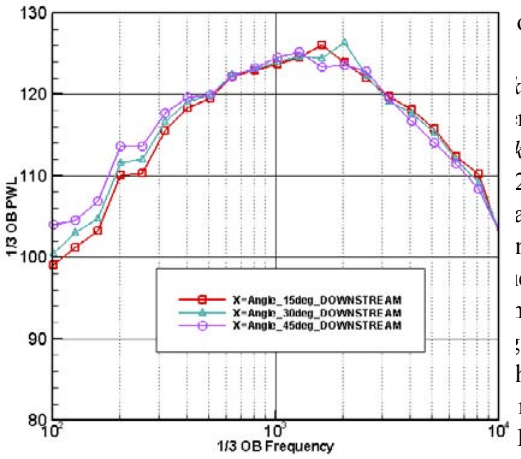

(b)

Fig. 6. Variation of acoustic power spectrum with stagger angle, θ. (a) upstream and (b) downstream.

ocities: in spectrum k_3 modes, nce spec- k_3 modes 2). There- agnitudes. ncy are of ency roll- ne present ; the two- he spectra model, is

4. Comp...

Using the 3-D formula derived in the last section, the broadband acoustic power spectrum can be calculated. In this section, a comparison between predicted acoustic power spectrum and a

presented to sources three-dime mean flow angle. The in Table provide a perimenta

Althougl by the Lie tensity and tic power Figure 3.

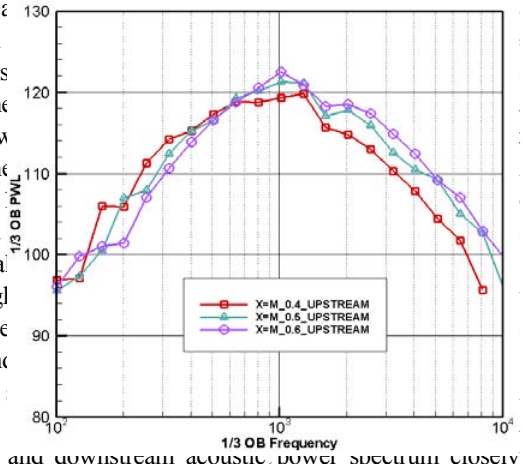

(a)

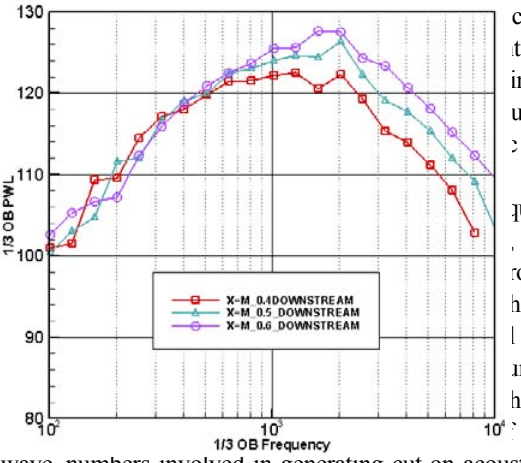

(b)

Fig. 7. Variation of acoustic power spectrum with Mach number, M. (a) upstream and (b) downstream.

ct that the ts of inci- ing to the ugmented. : field are of three- quency in- , which is roach used h a three- l spanwise um at zero hase along spanwise

upstream and downstream acoustic power spectrum closely matches experimental data.

5. Comparison with 2-D result

In Fig. 4, acoustic power spectra predicted using the present three-dimensional model are compared with those using the previous two-dimensional formulation [7, 8]. The parameters used in this calculation followed the baseline case used in the last section, shown in Table 1, except that the mean square value of turbulence velocity $\overline{w}^2$ was changed to $\overline{w}^2/W^2 = 4\times10^{-4}$. Note that the difference in magnitudes between the three-dimensional and two-dimensional spectra is wave numbers involved in generating cut-on acoustic waves and thus contributing to acoustic power is the same and independent of the frequencies for two dimensional cases. This difference characterizes the broadband noise due to the interaction between the turbulence and rectilinear cascade, compared with its corresponding two-dimensional one. Important implication of this finding is that the high-frequency approximate expression, proposed by Cheong et al. [7] to effectively predict the acoustic power spectrum due to turbulence-cascade interaction, can be still applied for the prediction of acoustic power spectrum due to this three-dimensional interaction.

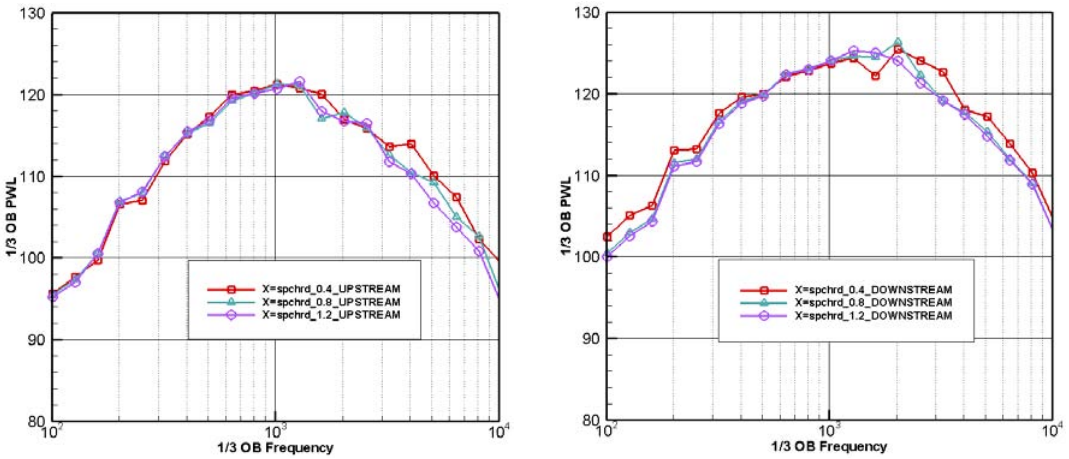

Fig. 8. Variation of acoustic power spectrum with gap-chord ratio, *s/c*. (a) upstream and (b) downstream.

6. Parametric studies

In this section, we examine the effect of different parameters on the acoustic power spectrum with a focus on the parameters of stagger angle θ, blade number B, Mach number M and gap-chord ratio s/c. For the parametric studies shown in this section, a baseline case is chosen to correspond to that used in Sec.V. This parametric study is a useful reference for stator designers.

Fig. 5 shows the variation of one-third octave band power levels for $B = 15, 30, 60$. In the high frequency range, approximately $f \geq 1000\ Hz$, the acoustic power both upstream and downstream is observed to be proportional to B, the same as that observed in the two-dimensional cases of works [7, 8].

Fig. 6 shows the power spectrum for the stagger angles of 15^o, 30^o and 45^o. At the high frequency range, the acoustic power upstream is observed to be proportional to stagger angle, while the downstream shows an opposite phenomenon. However, the effect of stagger angle on the downstream spectrum is generally small, particularly at high frequencies.

Fig. 7 shows the power spectrum for the Mach numbers of 0.4, 0.5 and 0.6. At the high frequency range, the acoustic power both upstream and downstream is observed to increase with Mach number, of which the reason is attributed mainly to the convection effect, as given in Eq. (20).

Fig. 8 shows the power spectrum for the gap-chord ratio $s/c = 0.4$, 0.8 and 1.2. As the approximate expression of Eq. (42) in Ref. [7] predicts that the sound power is independent of gap-chord ratio (or solidity) above the critical frequency, chord length has little effect on sound radiation. However, at the high frequency range, as gap-chord ratio increases, the acoustic power both upstream and downstream is observed to slightly decrease.

A similar parametric study is carried by Cheong et al. [7] under the same condition. The trends with various parameters obtained here closely match those obtained by Cheong et al. [7] who used two-dimensional theory, especially at high frequencies. The reason for this can be explained by the descriptions given in Section III.

7. Conclusions

Characteristics of the acoustic power spectrum, upstream and downstream of a three-dimensional cascade of flat plates bounded by two parallel walls impinging by isotropic frozen turbulent gusts have been investigated. The acoustic power spectrum formulation was derived, which includes the effects of span-wise wavenumber components of the impinging turbulent gust. This three-dimensional theory is based on the previous tonal noise theory of Smith [2] and its generalization to two-dimensional broadband noise theory by Cheong et al [7]. The validity of the present model is confirmed by comparing its prediction with the experiment.

Through the comparison of the acoustic power spectra predicted using the present three-dimensional model with those using the two-dimensional formula by Cheong et al. [7, 8], it is shown that the variation of the spectra with the frequencies comes to closer agreement between two predictions as the frequency increases, whereas there is significant difference of increasing rate of the spectra at lower frequencies. These results can be understood by noting the different dispersion relations between two- and three-dimensional acoustic fields. However, the closer agreements between the two models at higher frequencies allow the main findings provided in the previous works [7, 8] based on two-dimensional model to be valid and applied for the high-frequency three-dimensional broadband noise due to the interaction of the ingesting turbulence with the rectilinear cascade of flat plates bounded by two side walls. One of the most important implications is that the high-frequency approximate expression previously developed for the acoustic power spectrum in two-dimensions is applicable for current three-dimensional problem.

Through the subsequent parameter study, we aim at finding the effect of different parameters such as stagger angle and blade number on the whole acoustic power. As discussed in the parametric study section, as Mach number and blade number increase, the acoustic power both upstream and downstream increases; with stagger angle increasing, the acoustic power upstream decreases while the downstream acoustic power increases; and with gap-chord ratio increasing, the acoustic power spectrum both upstream and downstream does not show significant differences. This can be utilized as the reference when designing the aero-engine fan.

Acknowledgment

This work was supported by National Research Foundation of Korea (NRF) grant funded by Korea government (MEST) (No. 2009-0052961). This subject was also supported by Ministry of Environment of the Republic of Korea as "The Eco-technopia 21 project".

Nomenclature

a : Sound speed
B : The number of airfoils in cascade
R : The span length of an airfoil
s : Blade spacing or entropy
t : Time
u : Velocity perturbation in x_1 direction
v : Velocity perturbation in x_2 direction
w : Velocity perturbation in x_3 direction
$w(y,t)$: Upwash velocity perturbation
U : Mean velocity in x_1 direction
V : Mean velocity in x_2 direction
W : Mean velocity in x_3 direction
A : Mean-flow speed
l : Acoustic mode number in the gap-wise direction
m : Vortical mode number in the gap-wise direction
j : Vortical mode number in the span-wise direction
r : Scattering index in gap-wise direction
M : Mach number of the mean-flow
k_i : Wave number of ingested turbulence gust in Cartesian coordinate system
ρ_0 : Mean-stream density
ρ : Perturbation density
P : Perturbation pressure
α : Wave number of the generated disturbance in the axial direction
β : Wave number of the generated disturbance in the gap-wise direction
γ : Wave number of the generated disturbance in the span-wise direction
x_i : Cartesian duct coordinate system, Fig. 1
y_i : Cartesian cascade-fixed coordinate system Fig. 1
θ : Stagger angle, $\tan^{-1}(V/U)$
σ : Interblade phase angle
ω : Angular frequency
λ : Reduced frequency
Φ_{ww} : Turbulence spectrum

Subscript

$+$: Upstream going acoustic wave
$-$: Downstream going acoustic wave

References

[1] T. F. Brooks, D. S. Pope and M. A. Marcolini, Airfoil self-noise and prediction, *NASA RP1218* National Aeronautics and Space Administration, USA (1989).
[2] S. N. Smith, Discrete frequency sound generation in axial flow turbomachines, *Reports and Memoranda* No.3709, Aeronautical Research Control Council, London (1972).

[3] D. S. Whitehead, Classical two-dimensional methods, in : M.F. Platzer, F.O. Carta (Eds.), *AGARD Manual on Aeroelasticity in Axial Flow Turbomachines, Unsteady Turbomachinery Aerodynamics (AGARD-AG-298)*, Vol. 1, Neuilly sur Seine, France (1987) Chapter 3.

[4] S. A. L. Glegg, The response of a swept blade row to a three-dimensional gust, *J. Sound Vib.* 227 (1999) 29-64.

[5] D. B. Hanson and K. P. Horan, Turbulence/cascade interaction: Spectra of inflow, cascade response, and noise, AIAA-98-2319 (1998).

[6] D. B. Hanson, Influence of lean and sweep on noise of rotor and stator cascade with inhomogeneous inflow turbulence including effects of lean and sweep, *NASA CR 2001-210762* (2001).

[7] C. Cheong, P. Joseph and S. Lee, High frequency formulation for the acoustic power spectrum due to cascade-turbulence interaction, *Journal of the Acoustical Society of America,* 119 (1) (2006) 108-22.

[8] C. Cheong, V. Jurdic and P.Joseph, Decomposition of modal acoustic power due to cascade-turbulence interaction, *J. Sound Vib.*, 324 (1-2) (2009) 57-73.

[9] M. E. Goldstein, *Aeroacoustics*, McGraw-Hill, New York (1976).

[10] R. K. Amiet, Acoustic radiation from an airfoil in a turbulent stream, *J. Sound Vib.,* 41 (4) (1975) 407-420.

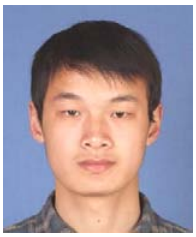

Dingbing Wei received his B.S. in Mechanical Engineering from Southeast University, China, in 2008; then continued his study as a graduate student in Pusan National University, Korea. He received his M.S. in Mechanical Engineering from Pusan National University in 2010. His main research interest is on inflow broadband fan noise.

Cheolung Cheong received his B.S. in Aerospace Engineering from Seoul National University in 1997. He received his M.S. and Ph. D. degrees in Mechanical and Aerospace Engineering from Seoul National University in 1999 and 2003. He is now an associate professor at the School of Mechanical Engineering at Pusan National University in Pusan, Korea. Dr. Cheong's current research interests include fan broadband noise, wind turbine noise, and computational aeroacoustics.